

Electronic Supplementary Information

Canopied *trans*-chelating bis(*N*-heterocyclic carbene) ligand: synthesis, structure and catalysis

Brad P. Morgan, Gabriela A. Galdamez, Robert J. Gilliard, Jr. and Rhett C. Smith*

Department of Chemistry and Center for Optical Materials Science and Engineering Technologies (COSMET), Clemson University, Clemson, SC 29634

Email: rhett@clemson.edu

List of Supporting Information Figures:

- Figure S1.** ^1H NMR spectrum of $[\text{Ag}(\mathbf{1})]\text{AgBr}_2$ (DMSO, 300 MHz)
- Figure S2.** Aromatic region of the ^1H NMR spectrum of $[\text{Ag}(\mathbf{1})]\text{AgBr}_2$ (DMSO, 300 MHz)
- Figure S3.** Aliphatic region of the ^1H NMR spectrum of $[\text{Ag}(\mathbf{1})]\text{AgBr}_2$ (DMSO, 300 MHz)
- Figure S4.** ^1H - ^1H Correlated Spectrum (COSY) of $[\text{Ag}(\mathbf{1})]\text{AgBr}_2$ (DMSO, 300 MHz)
- Figure S5.** Nuclear Overhauser Effect Difference (NOE-DIFF) Spectrum of $[\text{Ag}(\mathbf{1})]\text{AgBr}_2$ (DMSO, 300 MHz) for protons resonating at 5.43 ppm
- Figure S6.** Nuclear Overhauser Effect Difference (NOE-DIFF) Spectrum of $[\text{Ag}(\mathbf{1})]\text{AgBr}_2$ (DMSO, 300 MHz) for protons resonating at 3.96 ppm
- Figure S7.** Carbon-13 NMR spectrum of $[\text{Ag}(\mathbf{1})]\text{AgBr}_2$ (DMSO, 75 MHz)
- Figure S8.** Aromatic region of the ^{13}C NMR spectrum of $[\text{Ag}(\mathbf{1})]\text{AgBr}_2$ (DMSO, 75 MHz)
- Figure S9.** Heteronuclear Multiple Quantum Coherence (HMQC) spectrum of $[\text{Ag}(\mathbf{1})]\text{AgBr}_2$ (300 MHz for ^1H , 75 MHz for ^{13}C , in DMSO)
- Figure S10.** Distortionless Enhancement by Polarization Transfer (DEPT-135) spectrum of $[\text{Ag}(\mathbf{1})]\text{AgBr}_2$ (DMSO, 75 MHz)
- Figure S11.** Aromatic region of DEPT-135 spectrum of $[\text{Ag}(\mathbf{1})]\text{AgBr}_2$ (DMSO, 75 MHz)
- Figure S12.** ^1H NMR spectrum of $[\text{H}_2\mathbf{1}]\text{Br}_2$ (DMSO, 300 MHz)
- Figure S13.** Aromatic region of the ^1H NMR spectrum of $[\text{H}_2\mathbf{1}]\text{Br}_2$ (DMSO, 300 MHz)
- Figure S14.** ^{13}C NMR spectrum of $[\text{H}_2\mathbf{1}]\text{Br}_2$ (CD_3CN , 75 MHz)
- Figure S15.** Aromatic region of the ^{13}C NMR spectrum of $[\text{H}_2\mathbf{1}]\text{Br}_2$ (CD_3CN , 75 MHz)
- Figure S16.** ^1H NMR spectrum of $[\text{Cl}_2\text{Pd}(\mathbf{1})]$ (CDCl_3 , 300 MHz)
- Figure S17.** Aliphatic region of the ^1H NMR spectrum of $[\text{Cl}_2\text{Pd}(\mathbf{1})]$ (CDCl_3 , 300 MHz)
- Figure S18.** Aromatic region of the ^1H NMR spectrum of $[\text{Cl}_2\text{Pd}(\mathbf{1})]$ (CDCl_3 , 300 MHz)
- Figure S19.** ^{13}C NMR spectrum of $[\text{Cl}_2\text{Pd}(\mathbf{1})]$ (CDCl_3 , 75 MHz)
- Figure S20.** Aromatic region of the ^{13}C NMR spectrum of $[\text{Cl}_2\text{Pd}(\mathbf{1})]$ (CDCl_3 , 75 MHz)
- Figure S21.** ESI-MS of $[\text{Cl}_2\text{Pd}(\mathbf{1})]$ with theoretical isotopic distributions for major peak sets

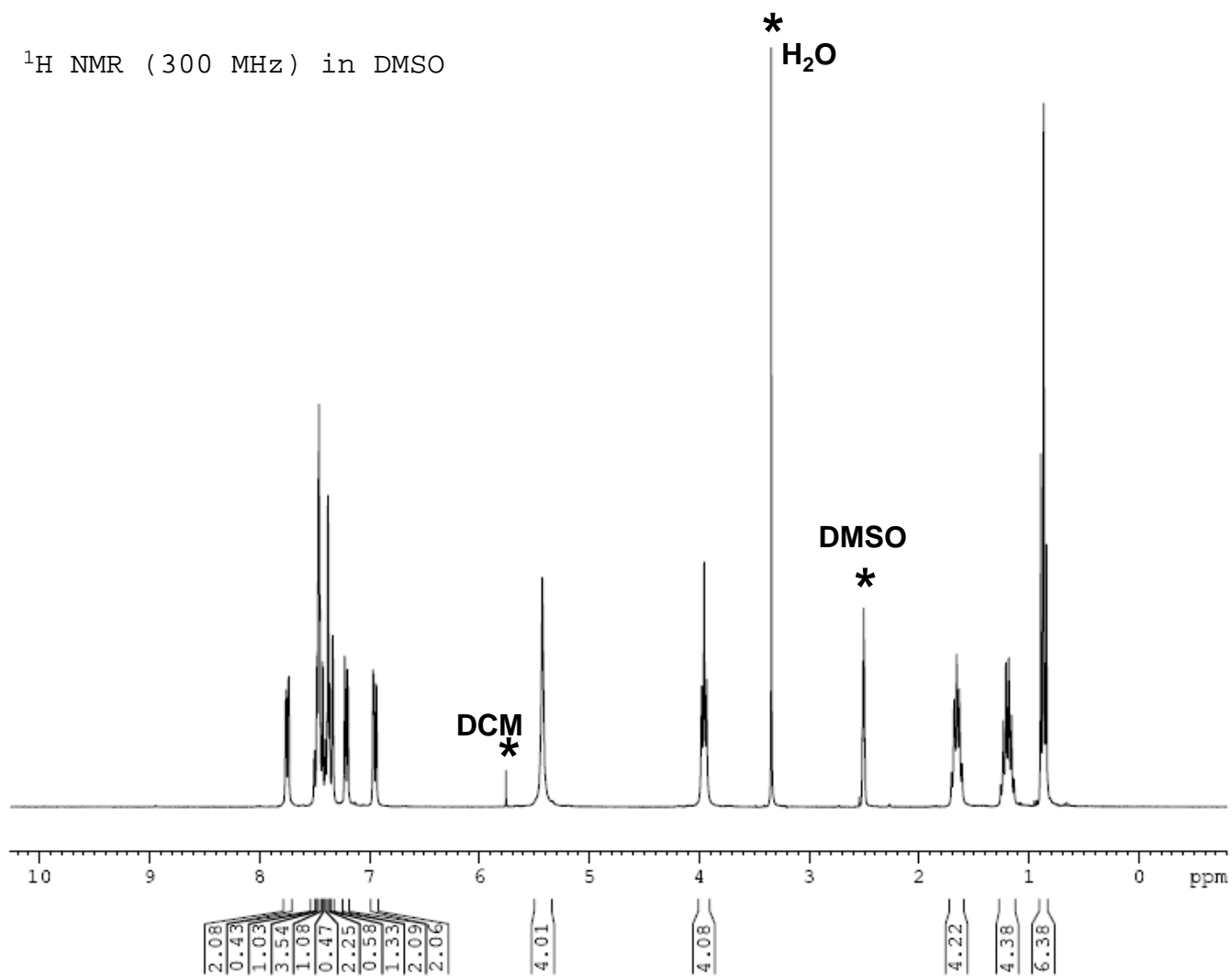


Figure S1. Proton NMR spectrum of $[\text{Ag}(\mathbf{1})]\text{AgBr}_2$ (DMSO, 300 MHz)

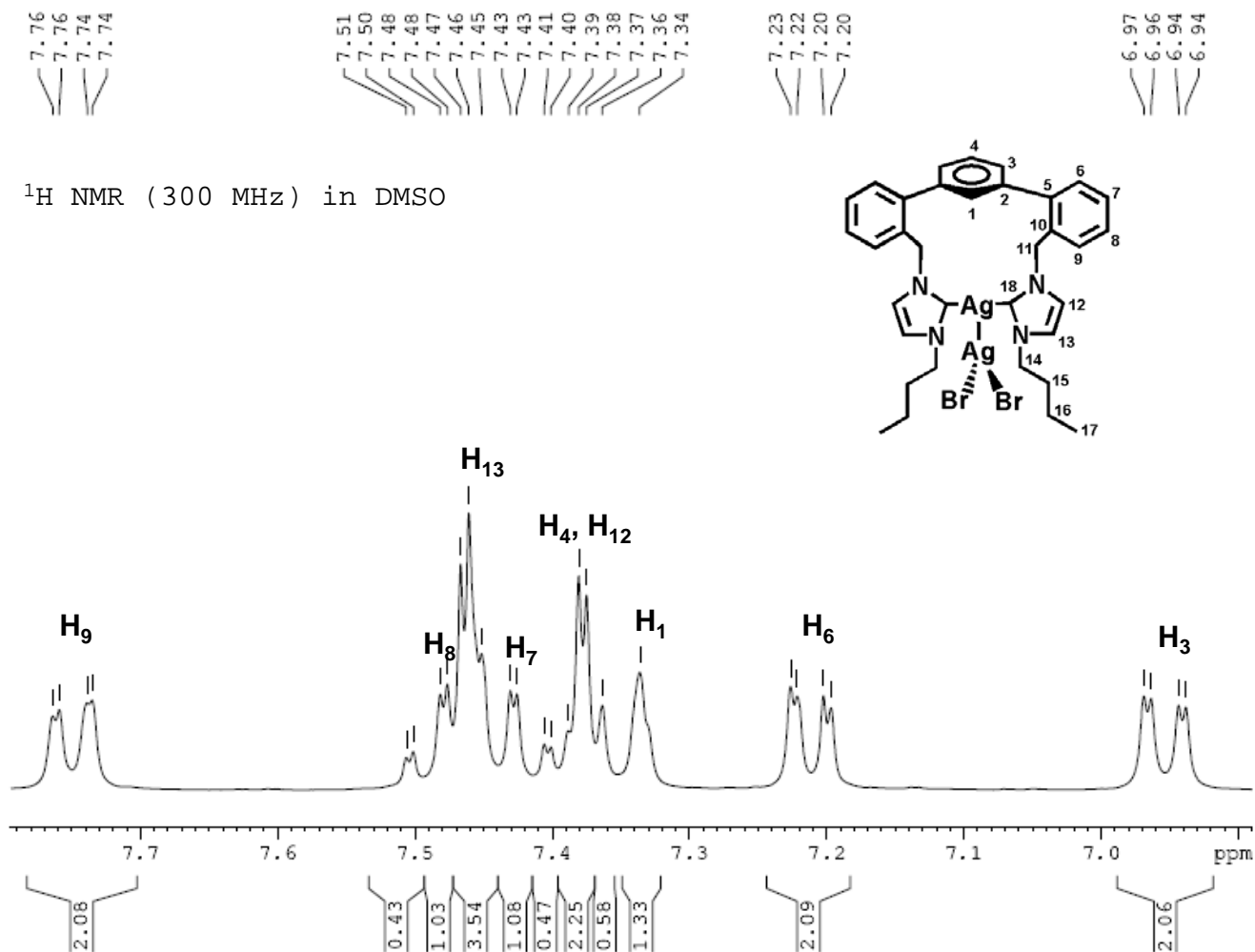


Figure S2. Aromatic Region of the ^1H NMR spectrum of $[\text{Ag}(\mathbf{1})]\text{AgBr}_2$ (DMSO, 300 MHz)

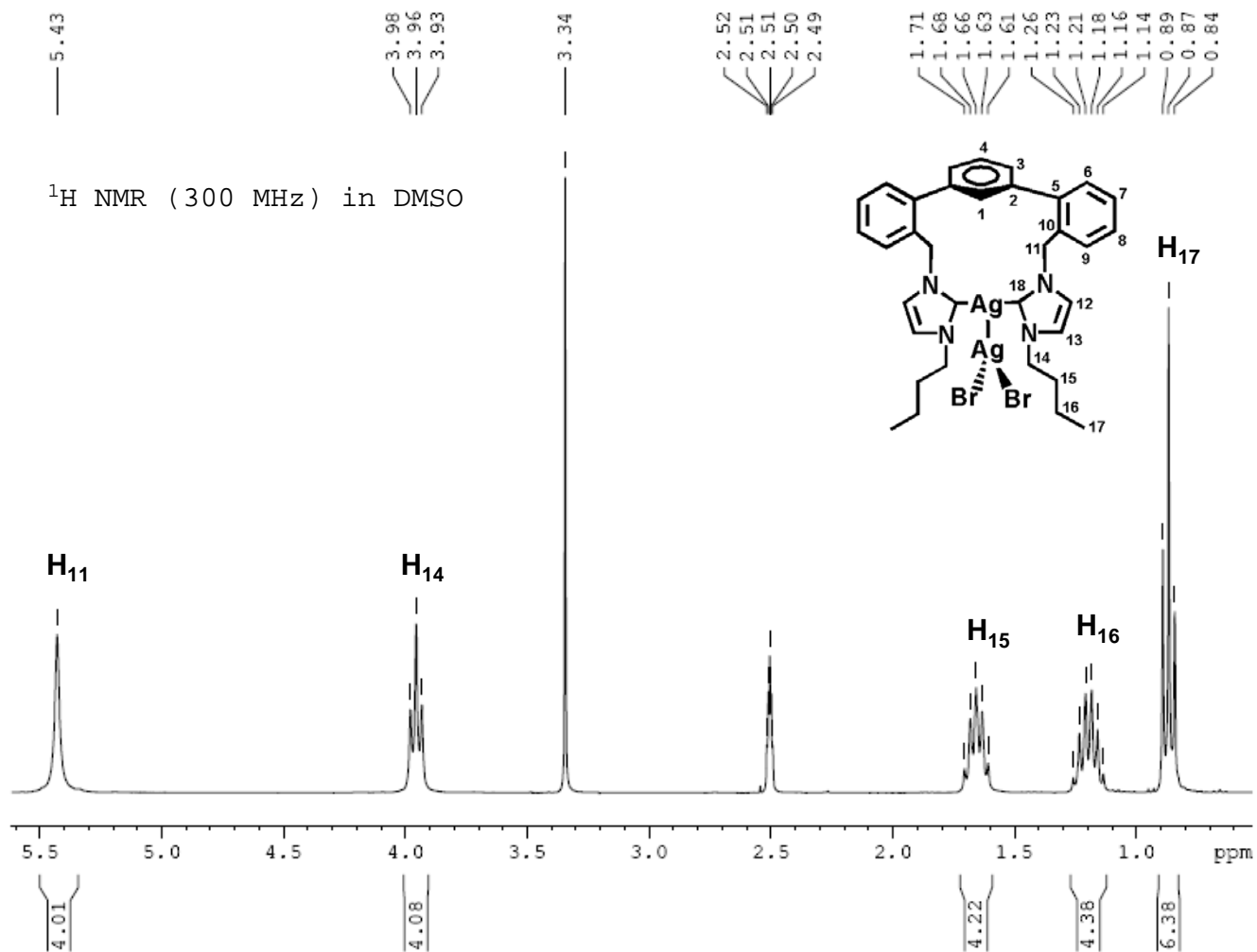


Figure S3. Aliphatic Region of the ^1H NMR spectrum of $[\text{Ag}(\mathbf{1})]\text{AgBr}_2$ (DMSO, 300 MHz)

^1H - ^1H COSY (300 MHz) in DMSO

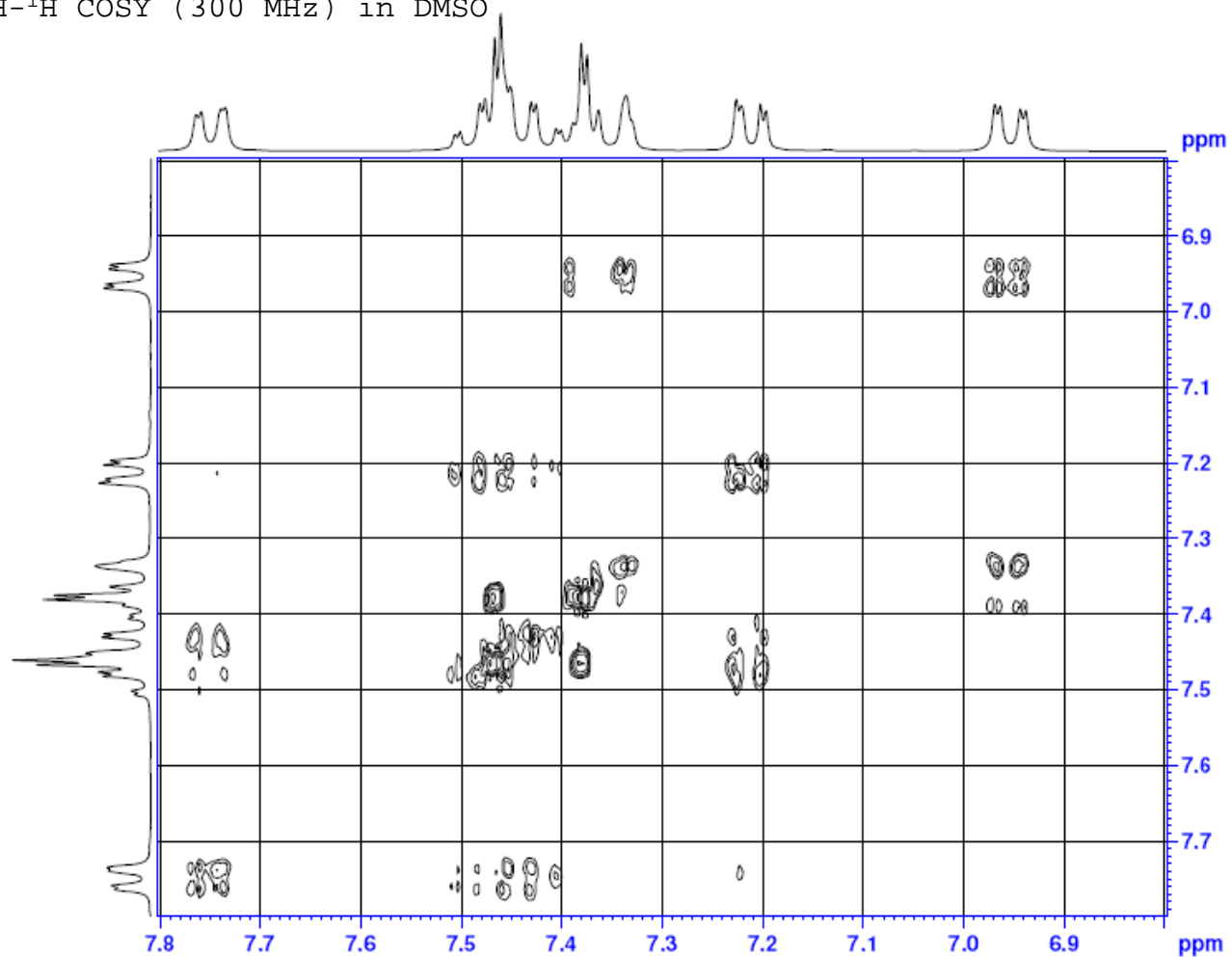


Figure S4. ^1H - ^1H Correlated Spectrum (COSY) of $[\text{Ag}(\mathbf{1})]\text{AgBr}_2$ (DMSO, 300 MHz)

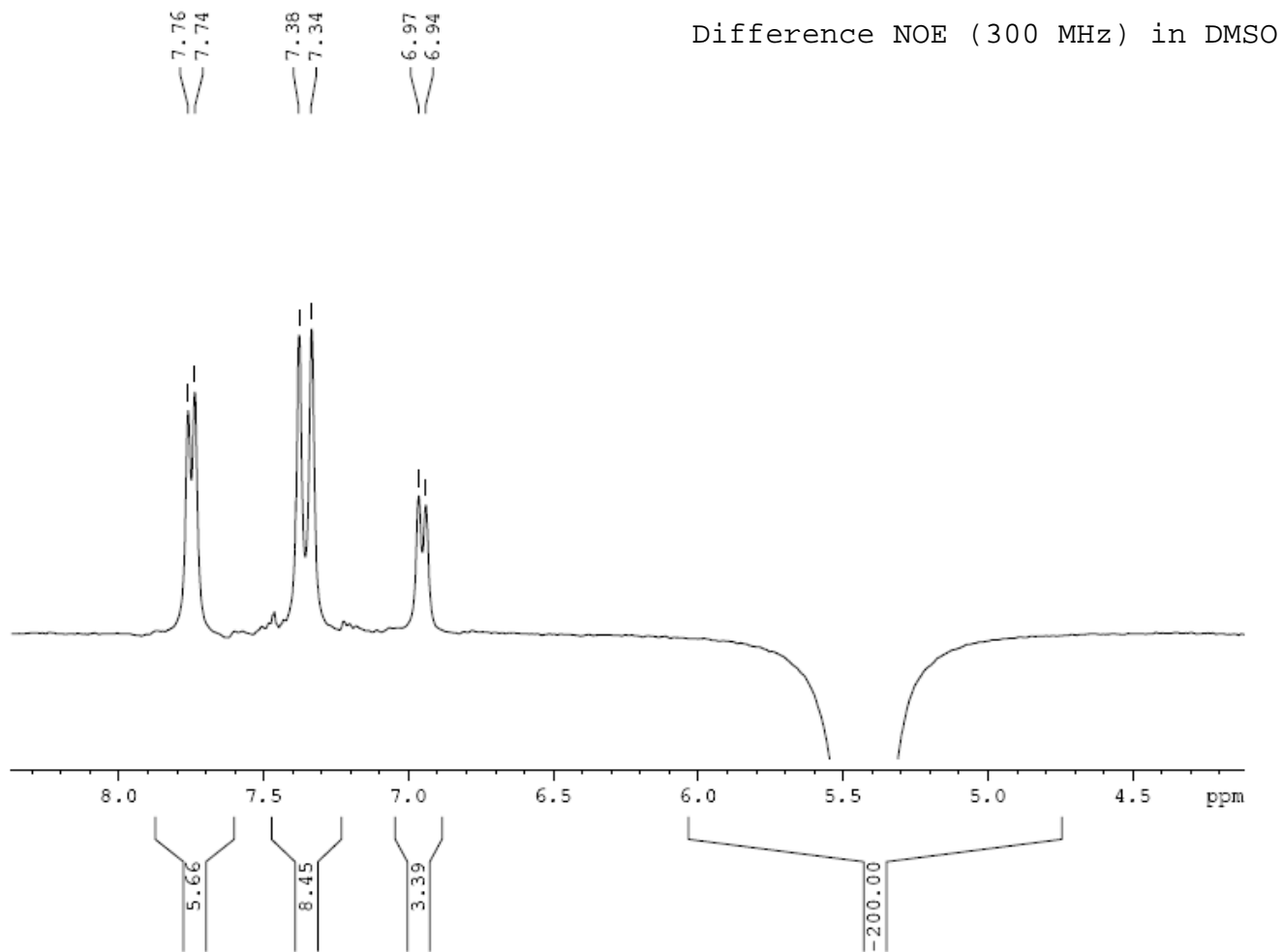


Figure S5. Nuclear Overhauser Effect Difference (NOE-DIFF) Spectrum of [Ag(1)]AgBr₂ (DMSO, 300 MHz) for protons resonating at 5.43 ppm

Difference NOE (300 MHz) in DMSO

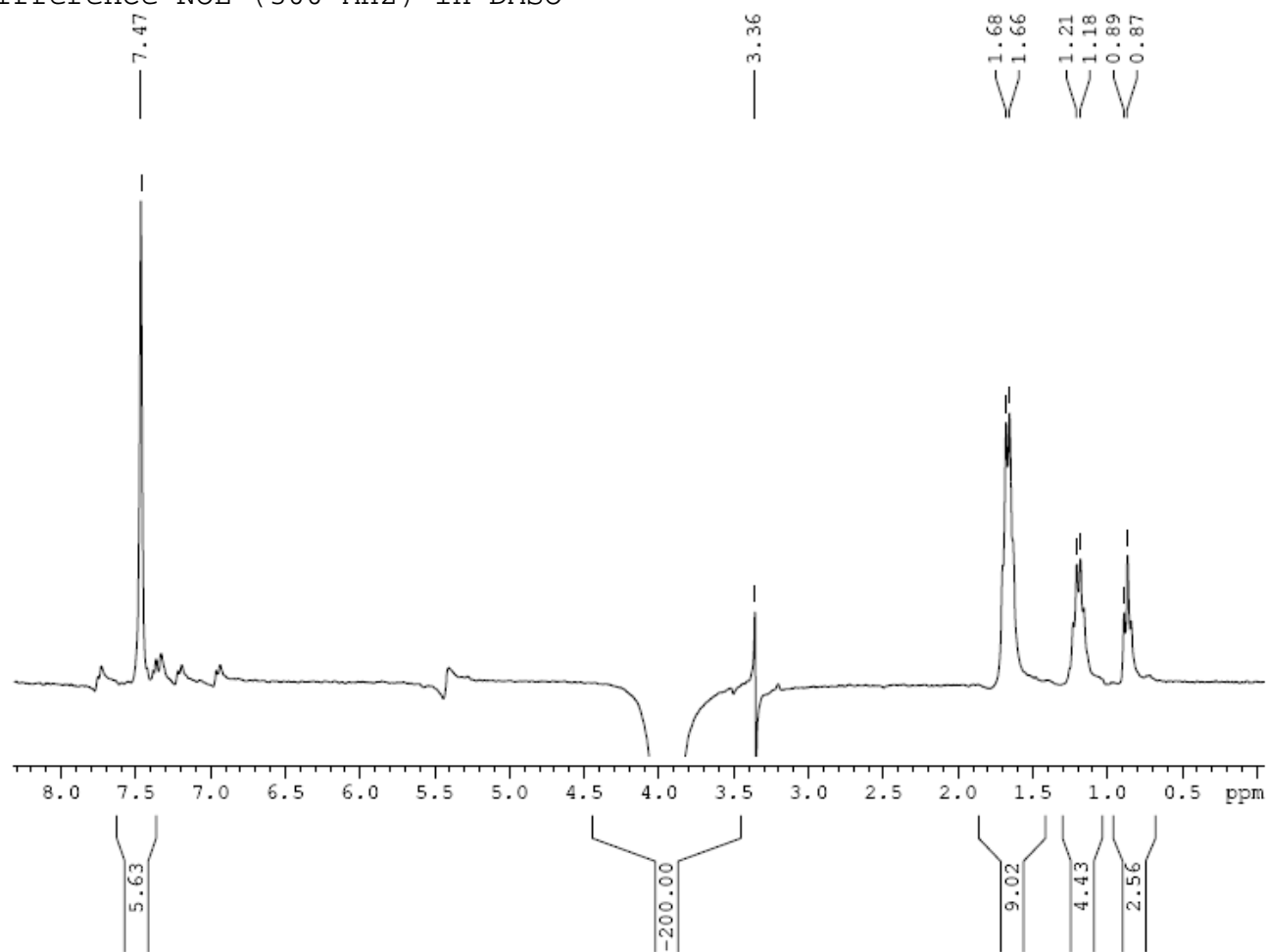


Figure S6. Nuclear Overhauser Effect Difference (NOE-DIFF) Spectrum of [Ag(1)]AgBr₂ (DMSO, 300 MHz) for protons resonating at 3.96 ppm

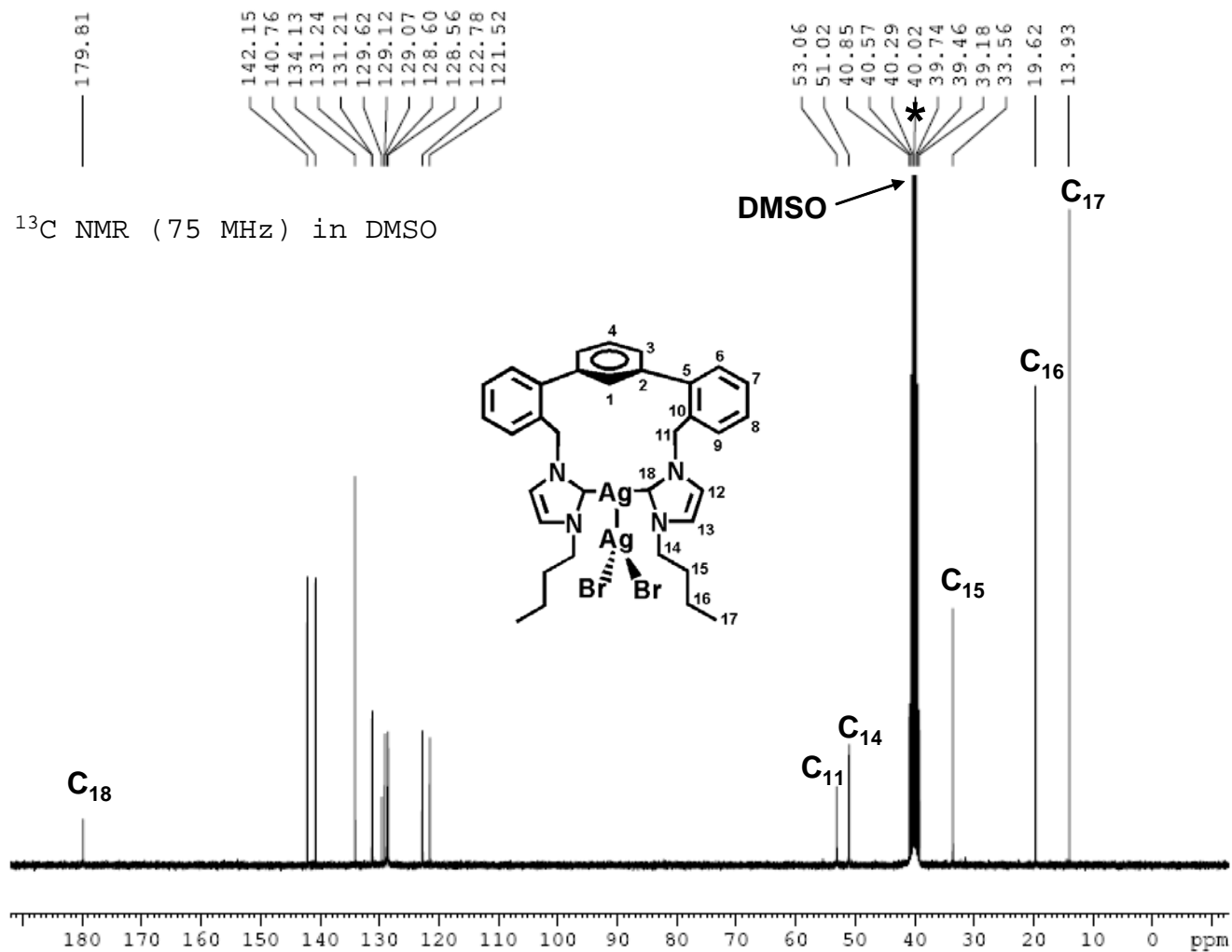


Figure S7. Carbon-13 NMR spectrum of [Ag(1)]AgBr₂ (DMSO, 75 MHz)

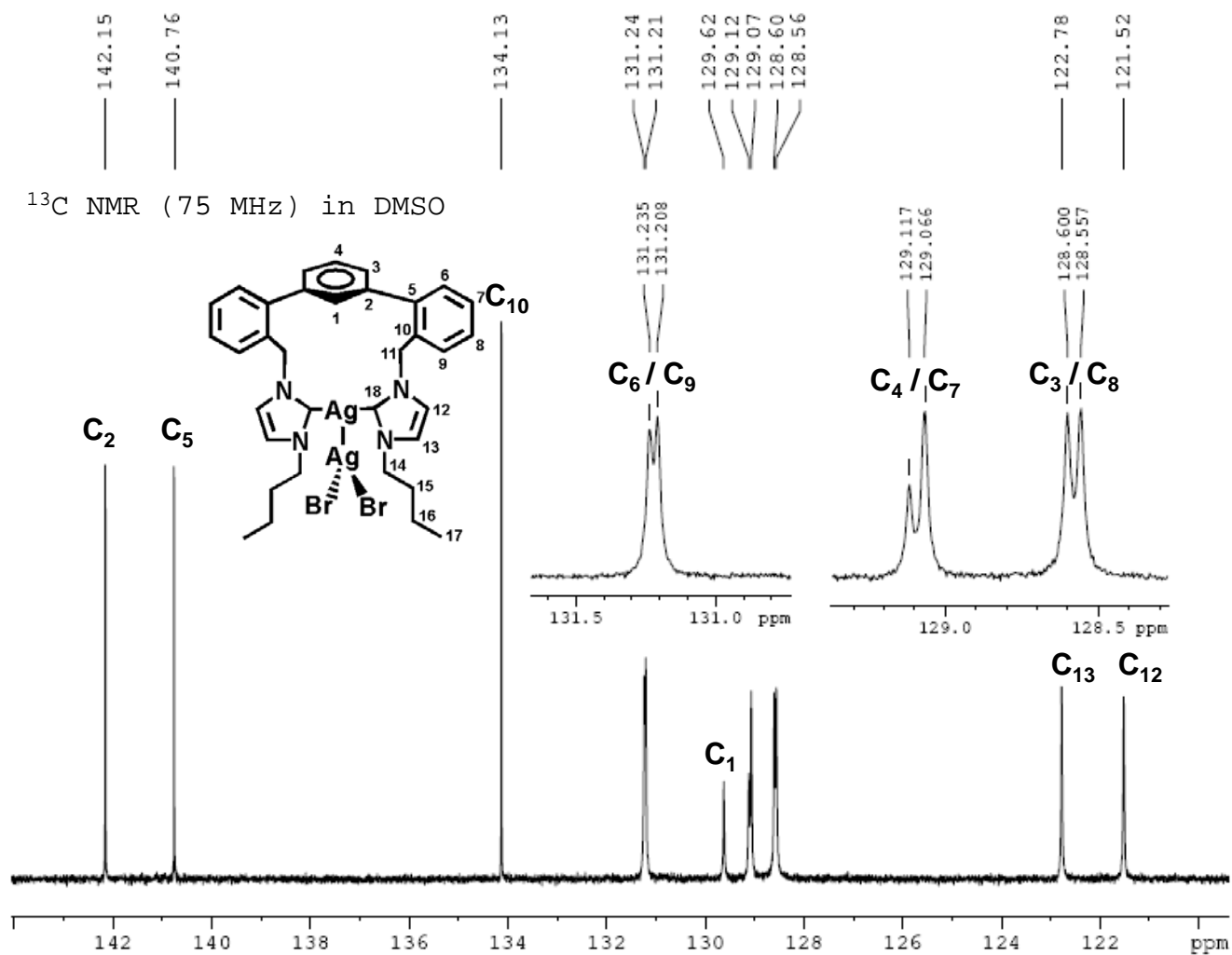


Figure S8. Aromatic region of the ^{13}C NMR spectrum of $[\text{Ag}(\mathbf{1})]\text{AgBr}_2$ (DMSO, 75 MHz)

HMQC (^1H , 300 MHz; ^{13}C , 75 MHz) in DMSO

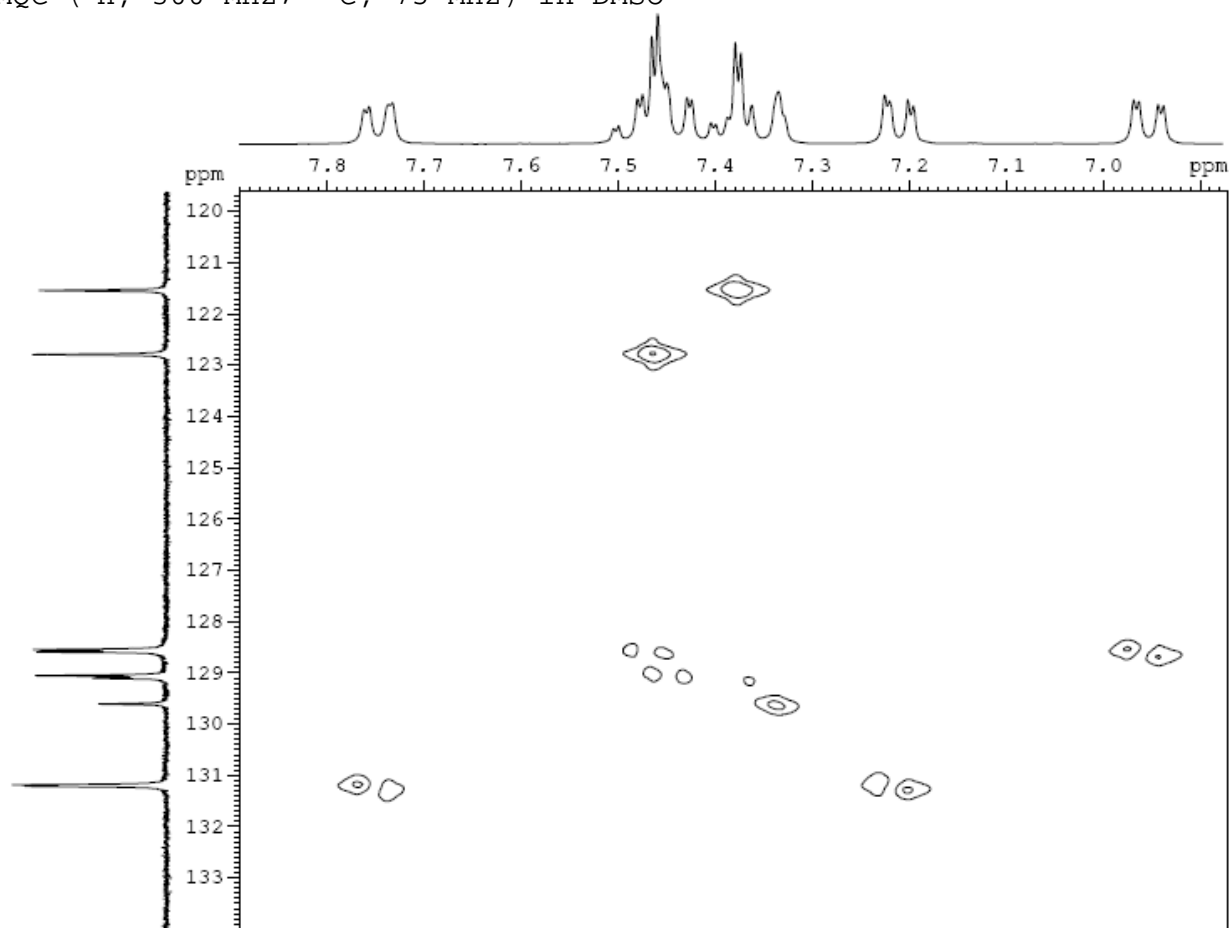


Figure S9. Heteronuclear Multiple Quantum Coherence (HMQC) spectrum of $[\text{Ag}(\mathbf{1})]\text{AgBr}_2$ (300 MHz for ^1H , 75 MHz for ^{13}C , in DMSO)

DEPT-135 (75 MHz) in DMSO

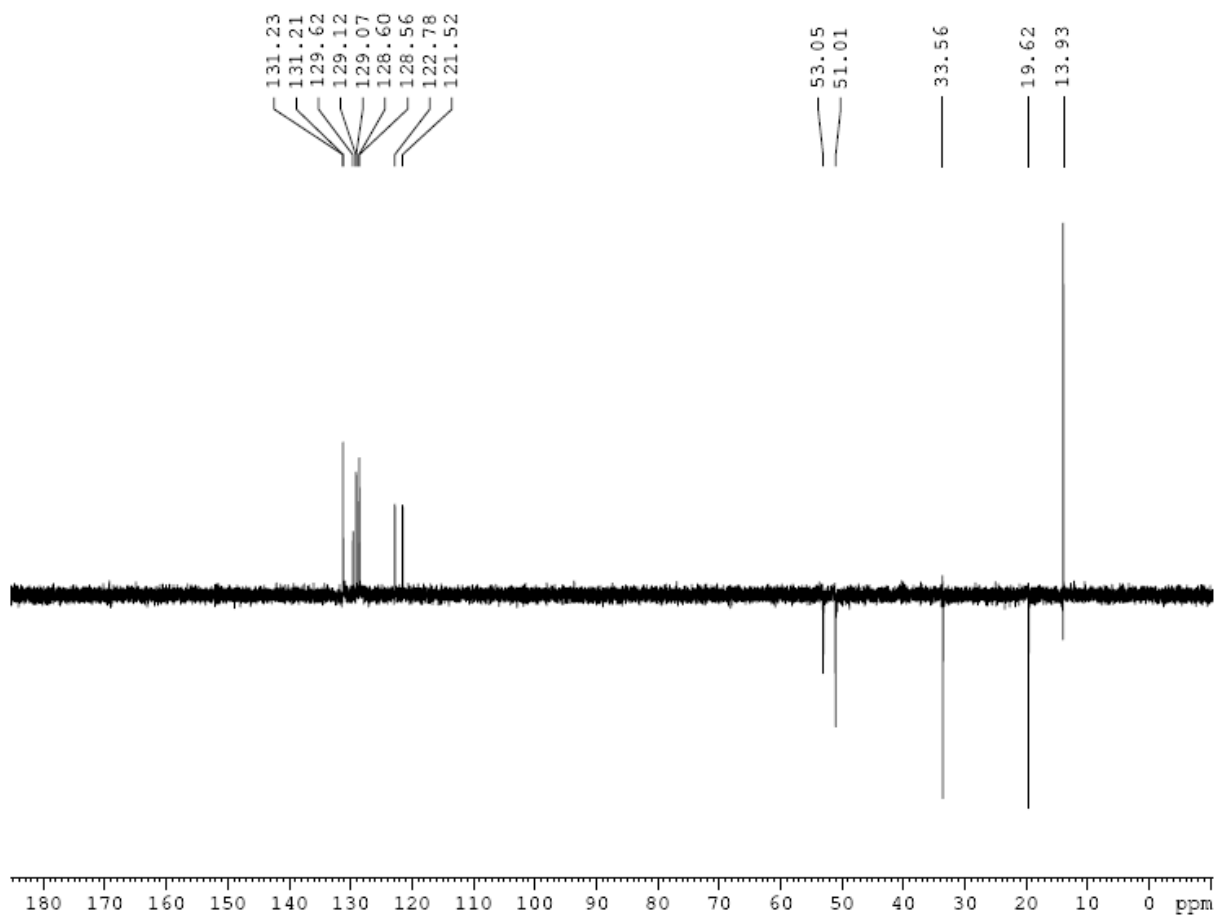


Figure S10. Distortionless Enhancement by Polarization Transfer (DEPT-135) spectrum of $[\text{Ag}(1)]\text{AgBr}_2$ (DMSO, 75 MHz)

DEPT-135 (75 MHz) in DMSO

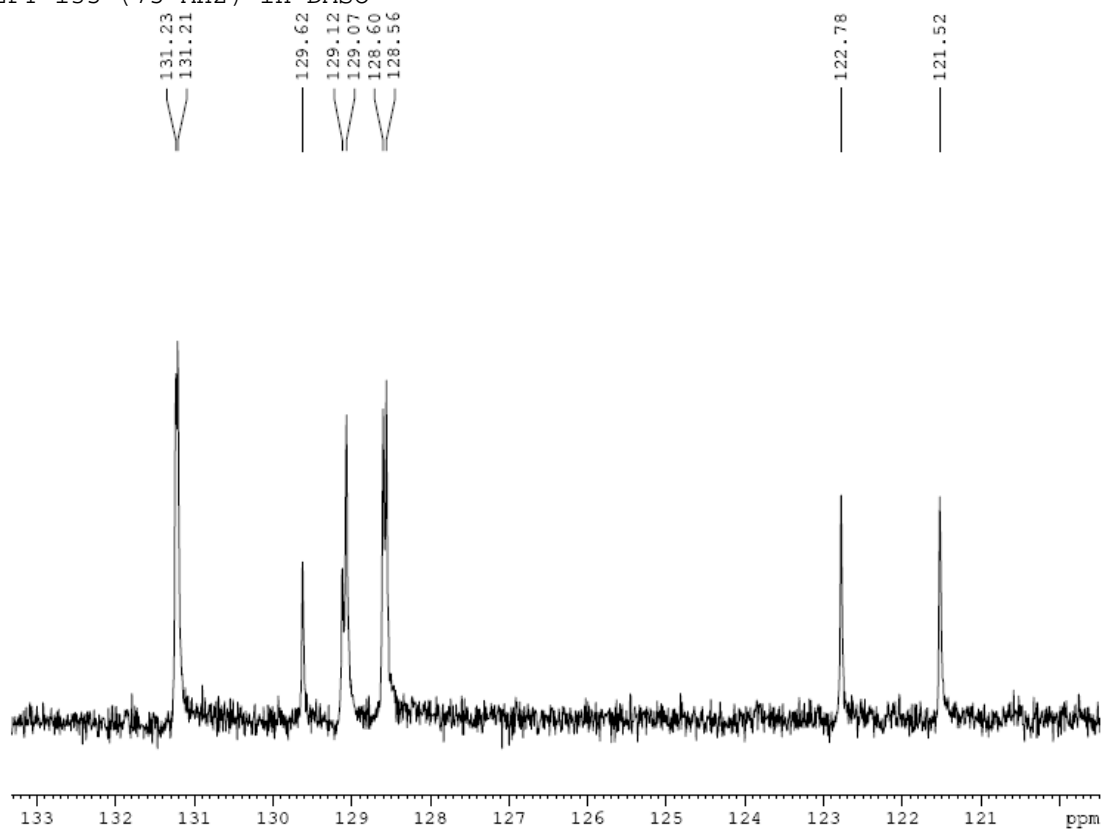


Figure S11. Aromatic region of DEPT-135 spectrum of [Ag(1)]AgBr₂ (DMSO, 75 MHz)

^1H NMR (300 MHz) in DMSO

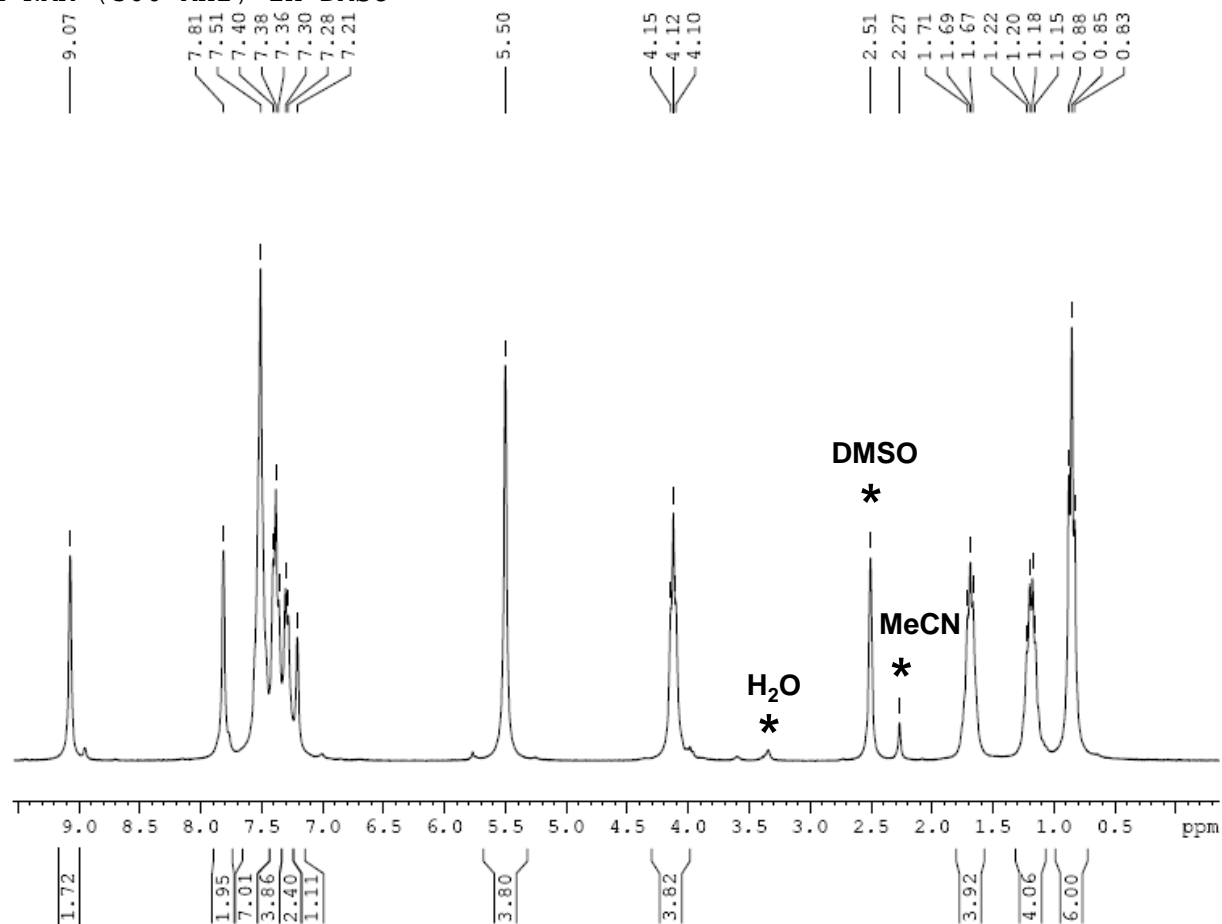


Figure S12. Proton NMR spectrum of $[\text{H}_{21}]\text{Br}_2$ (DMSO, 300 MHz)

^1H NMR (300 MHz) in DMSO

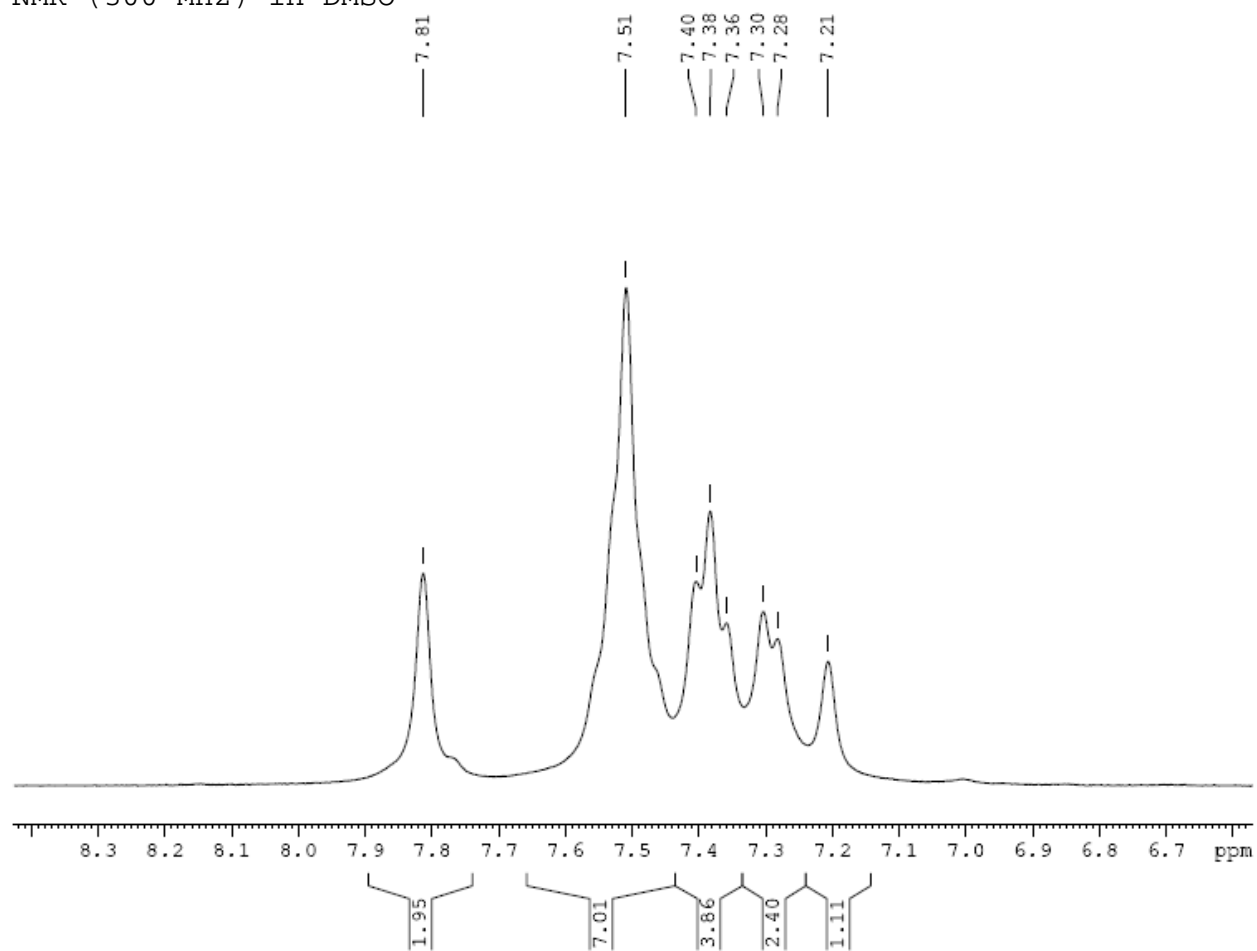


Figure S13. Aromatic Region of the ^1H NMR spectrum of $[\text{H}_2\mathbf{1}]\text{Br}_2$ (DMSO, 300 MHz)

^{13}C NMR (75 MHz) in CD_3CN

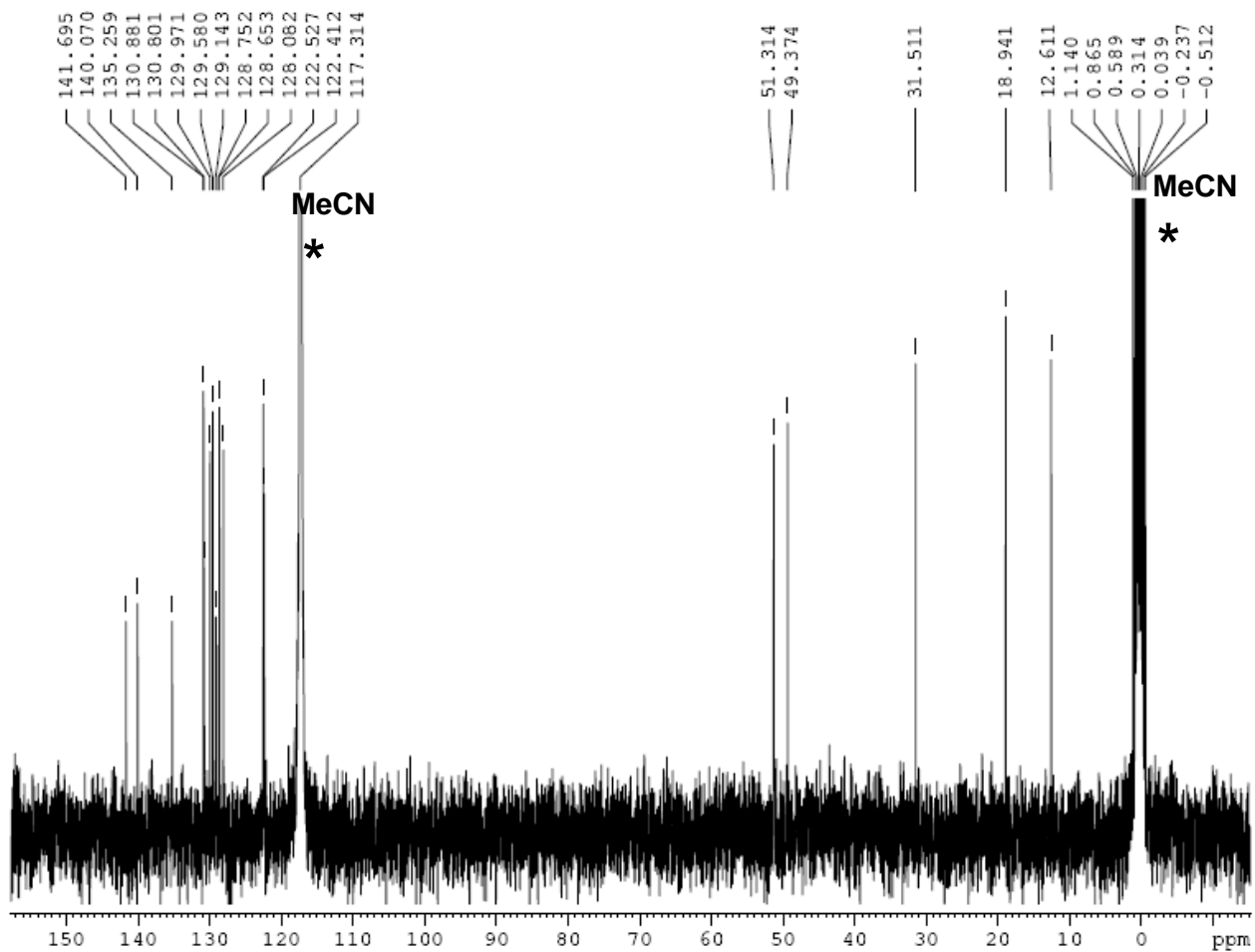


Figure S14. ^{13}C NMR spectrum of $[\text{H}_2^1]\text{Br}_2$ (CD_3CN , 75 MHz)

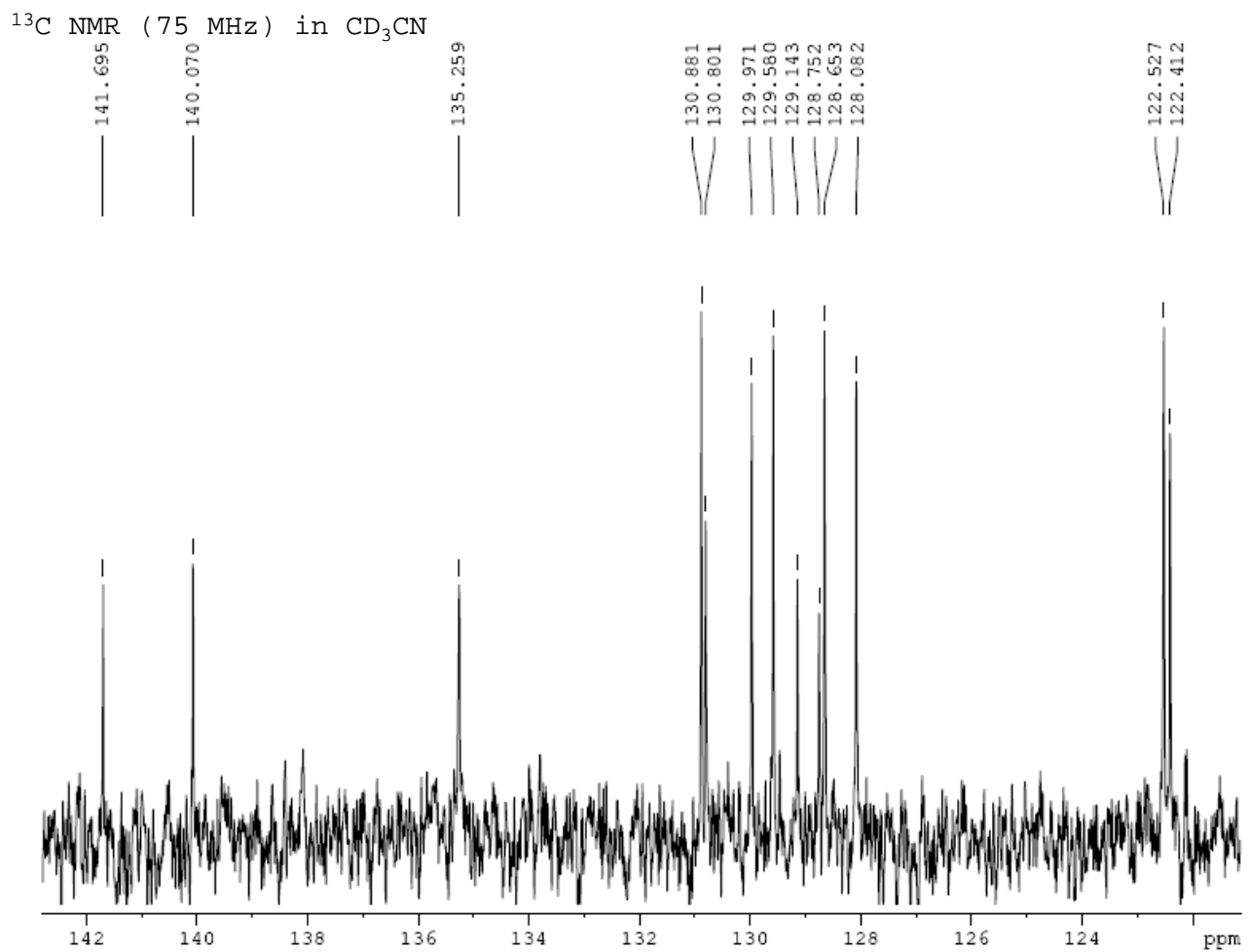


Figure S15. Aromatic region of the ^{13}C NMR spectrum of $[\text{H}_2\mathbf{1}]\text{Br}_2$ (CD_3CN , 75 MHz)

^1H NMR (300 MHz) in CDCl_3

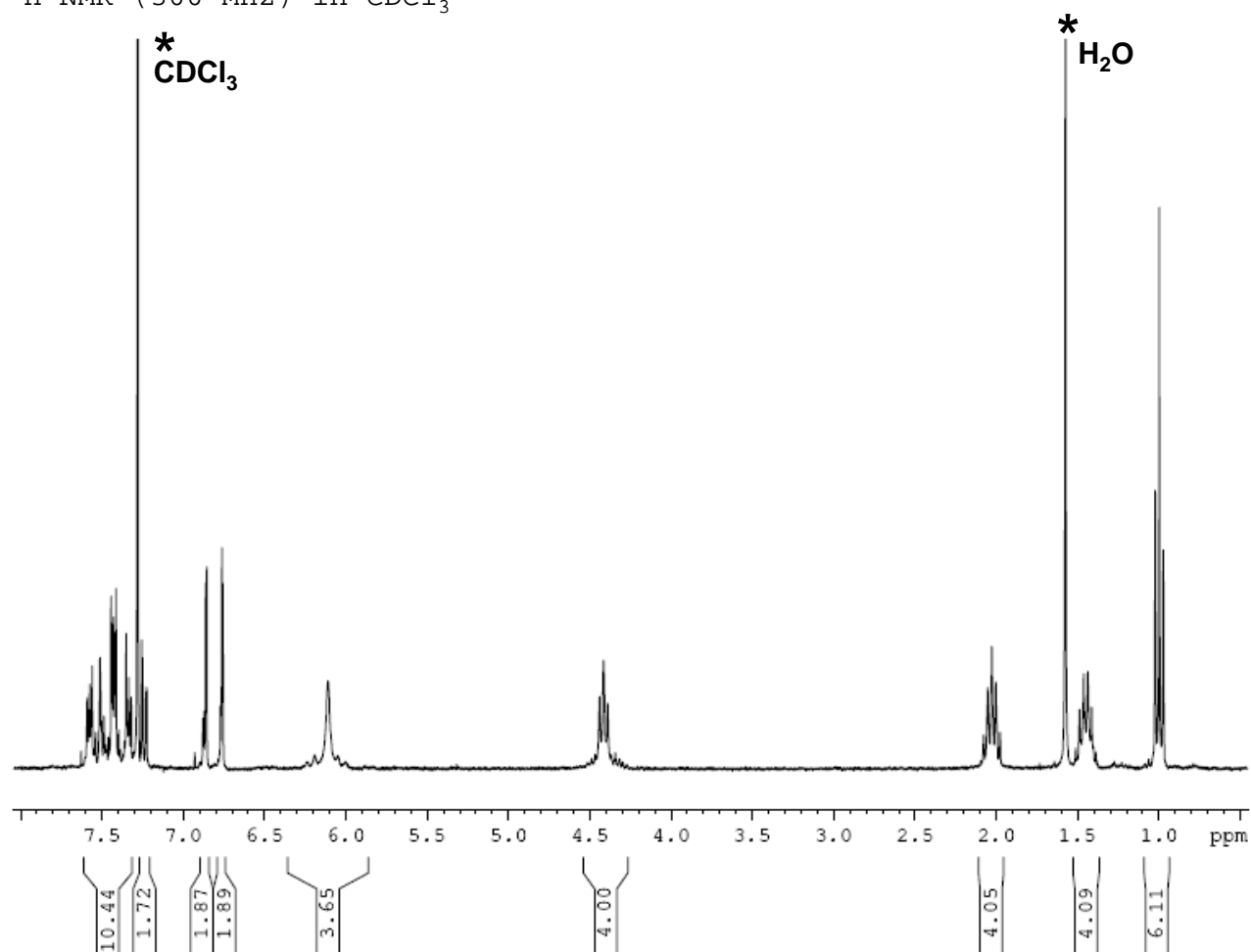


Figure S16. ^1H NMR spectrum of $[\text{Cl}_2\text{Pd}(\mathbf{1})]$ (CDCl_3 , 300 MHz)

^1H NMR (300 MHz) in CDCl_3

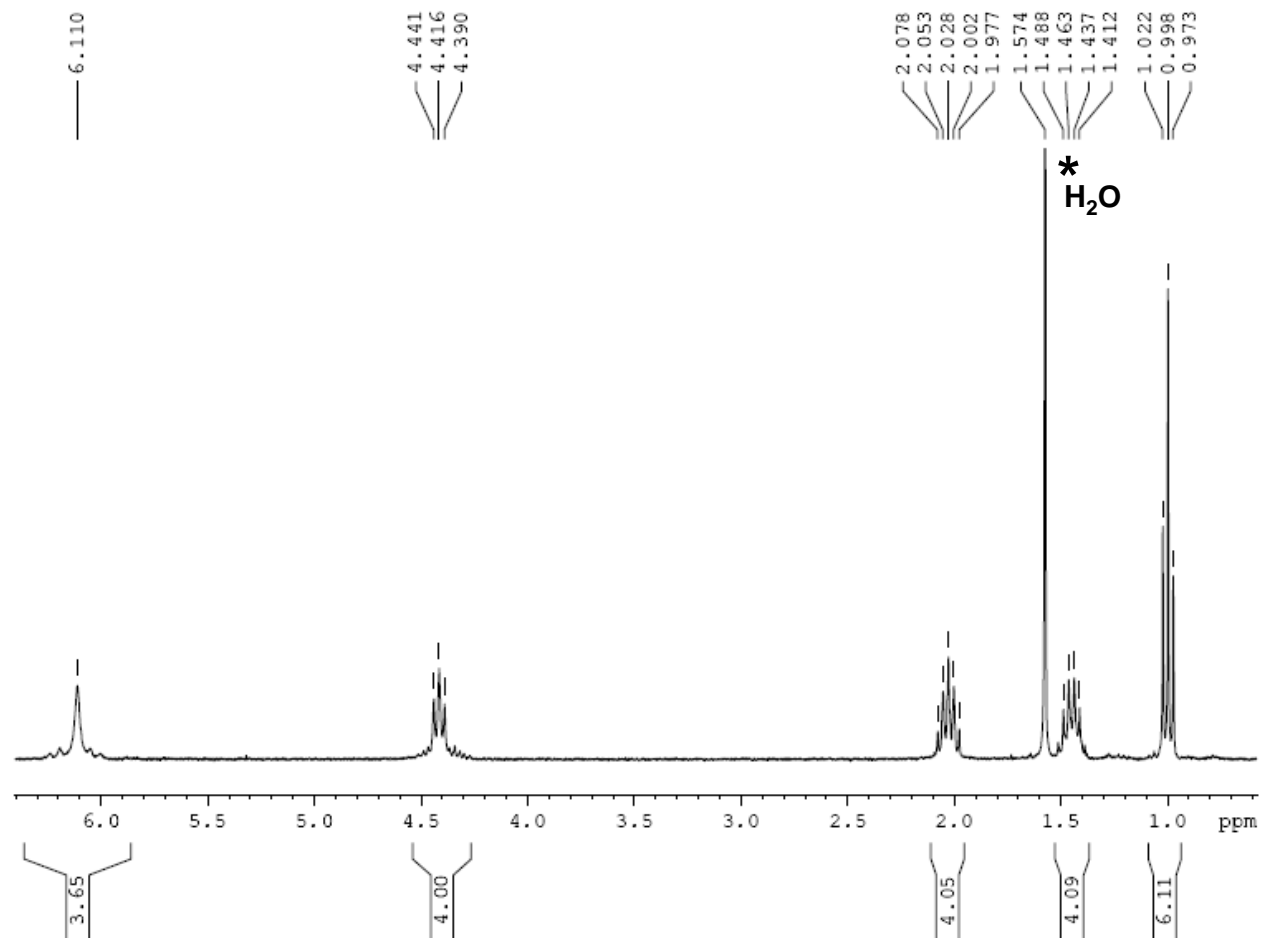


Figure S17. Aliphatic region of the ^1H NMR spectrum of $[\text{Cl}_2\text{Pd}(\mathbf{1})]$ (CDCl_3 , 300 MHz)

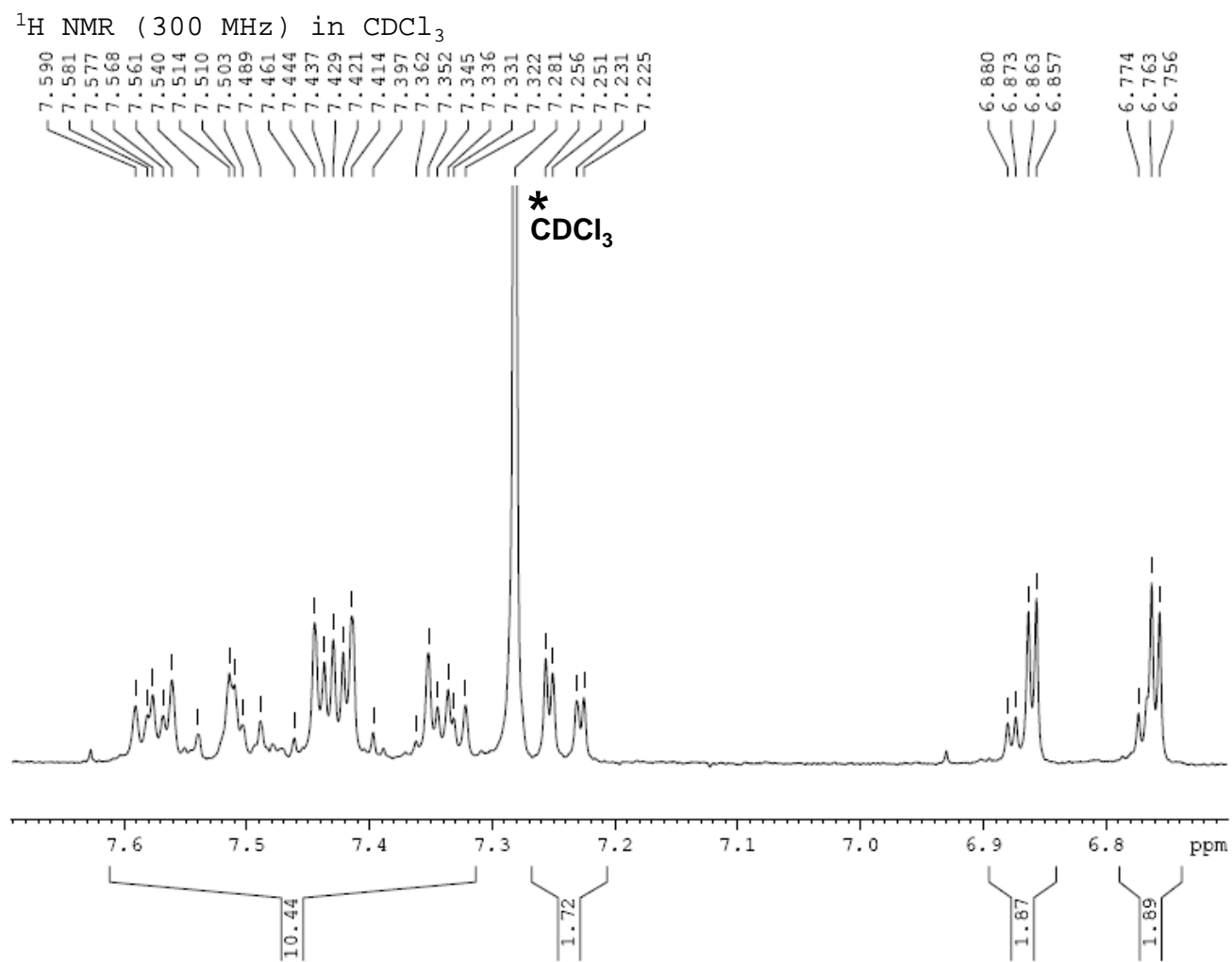


Figure S18. Aromatic region of the ^1H NMR spectrum of $[\text{Cl}_2\text{Pd}(\mathbf{1})]$ (CDCl_3 , 300 MHz)

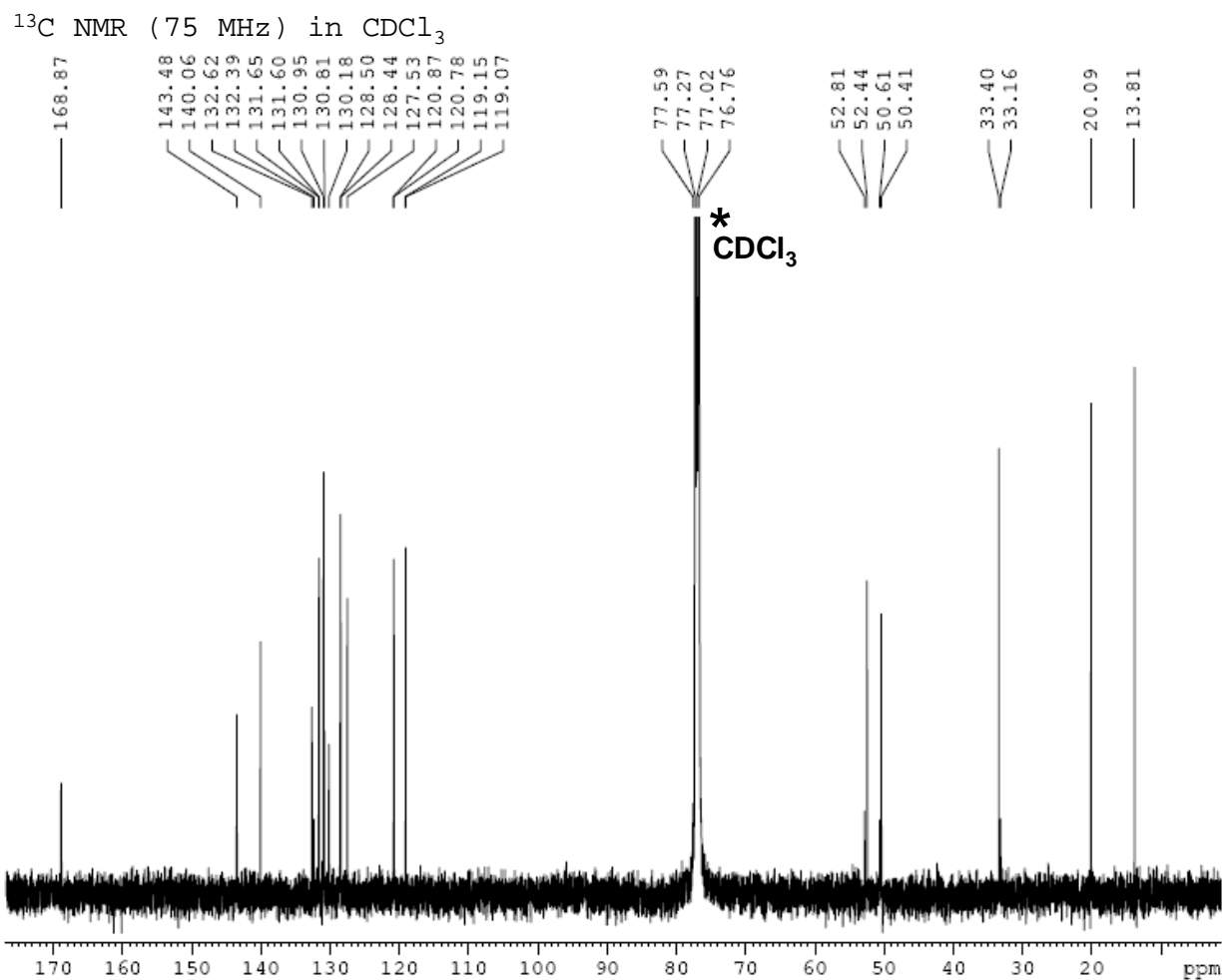


Figure S19. ^{13}C NMR spectrum of $[\text{Cl}_2\text{Pd}(\mathbf{1})]$ (CDCl_3 , 75 MHz)

^{13}C NMR (75 MHz) in CDCl_3

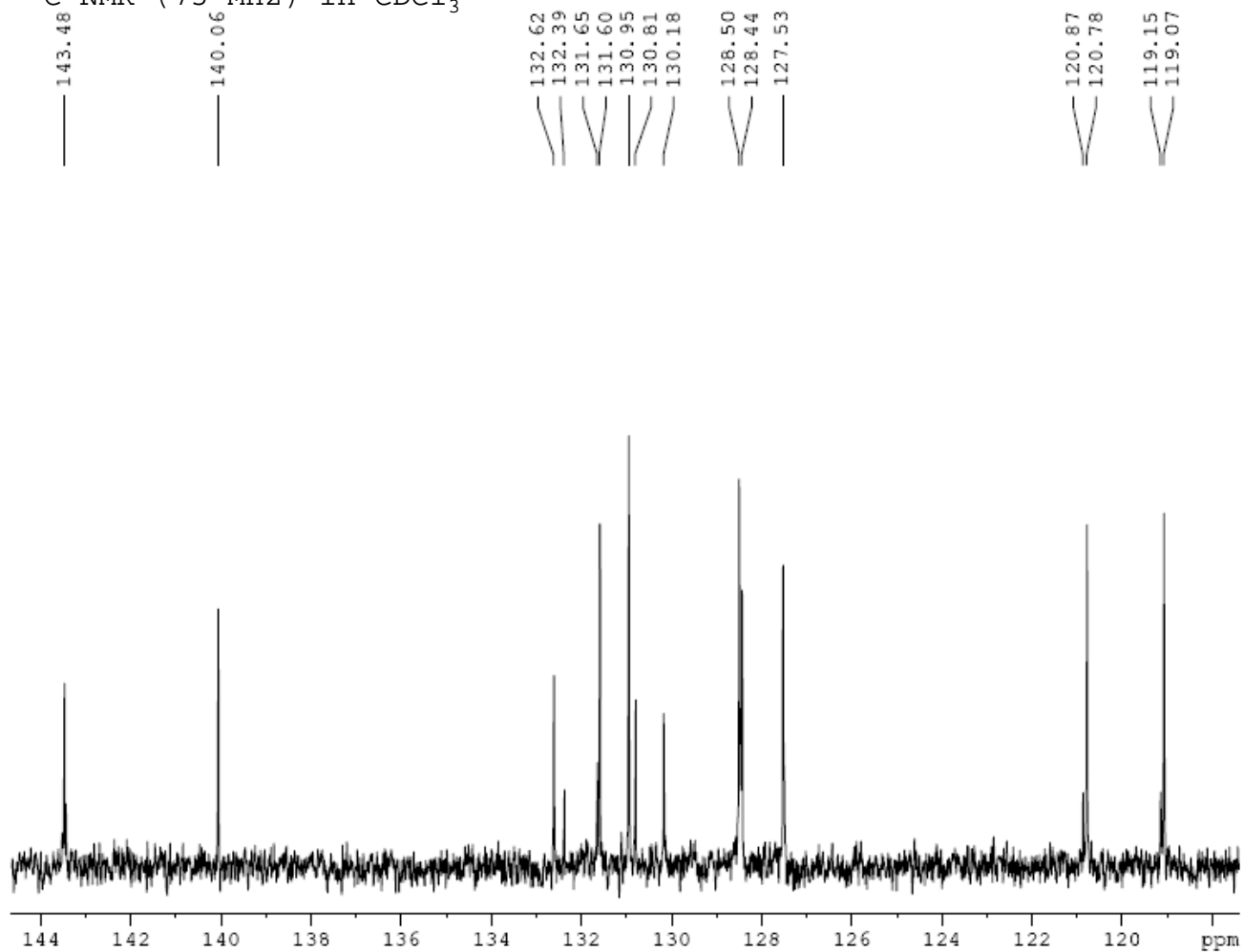


Figure S20. Aromatic region of the ^{13}C NMR spectrum of $[\text{Cl}_2\text{Pd}(\mathbf{1})]$ (CDCl_3 , 75 MHz)

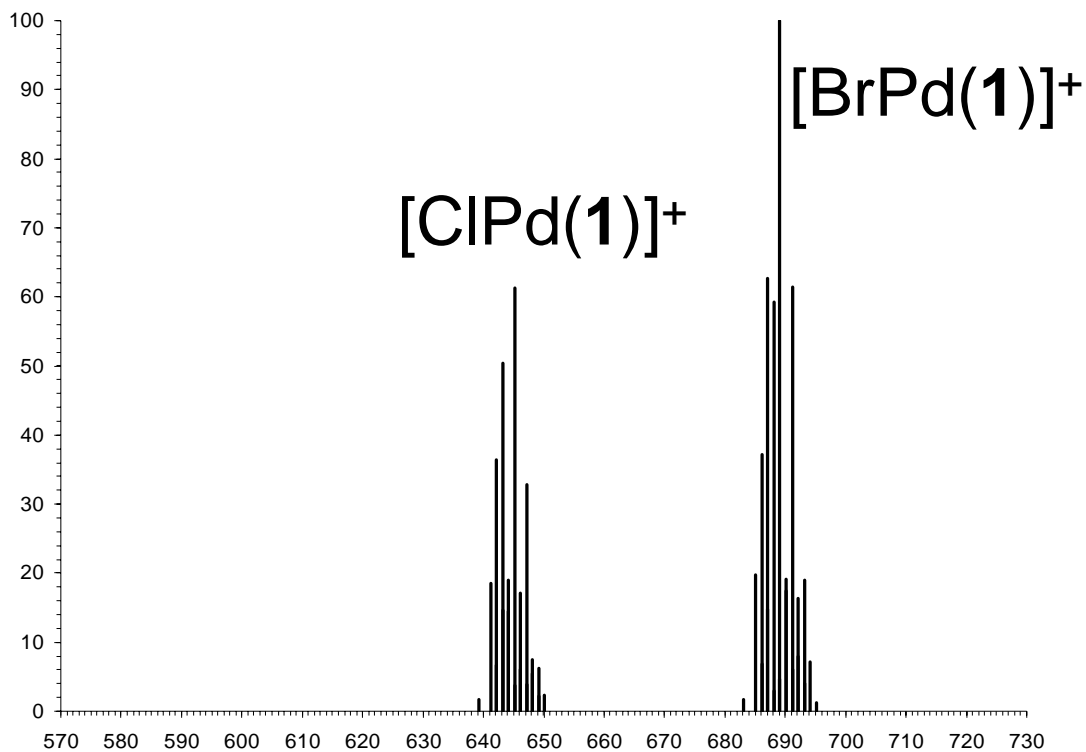
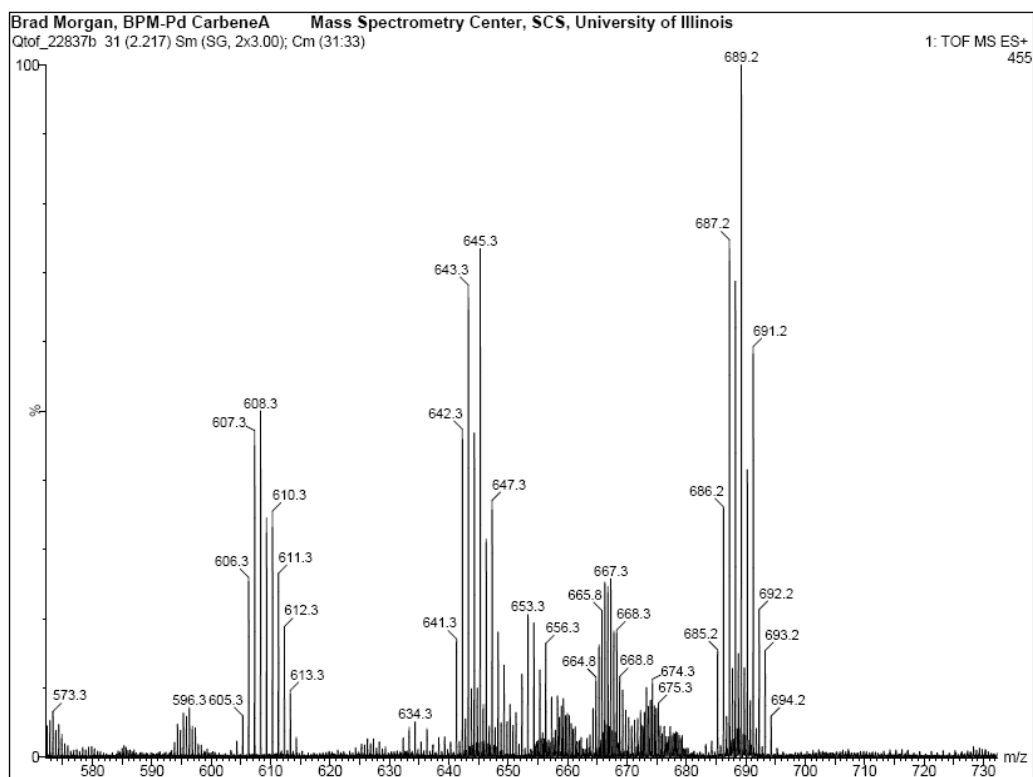


Figure S21. ESI-MS of $[\text{Cl}_2\text{Pd}(1)]$ (top) with theoretical isotopic distributions (bottom) for major peak sets